Robotics & Computer-Integrated Manufacturing, Vol. 9, No. 6, pp. 505–511, 1992
Printed in Great Britain

0736–5845/92 $5.00 + 0.00

● *Paper*

A CAD-BASED ERROR MAPPING AND LAYOUT FACILITY FOR PRECISION ROBOTIC OPERATIONS

Y. L. YAO* and M. R. MOHD YUSOFF†

* School of Mechanical and Manufacturing Engineering, University of New South Wales, Australia and
† Department of Mechanical Engineering, University of Wollongong, Australia

This paper describes development of a kinematic error mapping and layout facility for precision robotic operations such as a tight-tolerance assembly. The facility is based on a CAD system which models the robot geometry and allows robot models and associated equipment to be positioned into a working arrangement and viewed in three dimensions, along with the working envelope of the robot. Both nonlinear and linearized models are used, in conjunction with the CAD database, to predict the distribution of the end-effector errors over the working volume. The 3D error distribution is then displayed in terms of an error map, such that the spot(s) with the minimum error in a sense consistent with the nature of an operation can be chosen to carry out the operation or the robotic cell layout is altered. The facility is based on a "low cost" CAD package (AutoCAD) suitable for operation on a personal computer and the built-in AutoLisp language is fully made used of to automate graphics and facilitate error model calculations. The functionality of the system is illustrated with reference to a revolute 4-axis robot, and the development of a robotic material handling workcell. It is shown that using the facility not only reduces the technique risks one may encounter during the time-consuming trial and errors, but also makes possible extensive evaluations and compromises among various options which is essential in the layout and planning phase.

1. INTRODUCTION

A computer-aided layout and planning facility of manufacturing workcells involving industrial robots has been found essential for smaller manufacturing lots with more frequent model changes and volatile markets.[1–4] The advantages of such a layout and planning facility include: reduced technical risks; reduced downtime cost; reduced dependence on prototypes and in many cases prototypes do not even need to be manufactured before production; and many problems such as collisions can be avoided with less trial-and-error and greater confidence. With the advent of PC-based CAD packages capable of 3-D geometric modelling, animation, and sophisticated built-in programming capabilities, such a facility becomes more justifiable ever than before.

The functions of a computer-aided robotic layout and planning facility may include: (1) geometric modelling of robots and other equipment in one form or another; (2) analysis, optimization and evaluation; and (3) animation. The second function is the key to the system. It may include the capability to determine the optimum location of a robot within a manufacturing workcell[3] or to predict the error outcome of a robot in precision applications such as in assembly operations with a tight tolerance.

Many factors could influence the accuracy of robotic operations, such as the tolerance of the parts in mating, jigging and fixtures error, and errors in the robot itself. Among them the errors associated with the robot itself are most difficult to assess because they depend on robot configurations. Robotic errors can be divided into two types: kinematic errors and dynamic errors. Kinematic errors may result from imprecise manufacturing of robot links and joints and also from wear of the components once a robot is in operation. Encoder errors or offsets are also part of kinematic errors.[5]

Extensive research has been and is still being carried out in dealing with the kinematic errors of robots. Most of them identify the errors through a calibration procedure, either directly[5] or inversely.[6] In order to successfully identify theses errors, a proper error model structure has to be used. Some proposed linearized models for the four well-known kinematic parameters, while the others suggested similar models including the second order effects or the fifth parameter error for parallel axes.[7–14] From a practical point of view, it is often found that it is more desirable to know the "distribution" of the end-effector errors within the working envelope. Attempts have been made to plot the positioning accuracy as a surface.[15]

During the planning stage of robotic applications involving precision operations, such as part assembly with a tight tolerance, it is highly desirable for a human planner or a planning system to have a reliable

assessment of which location(s) of a robotic cell will give a greater accuracy in which the operation can be carried out with a higher success rate. The assessment is necessary because robot accuracy is a function of its configuration, therefore a function of location. However, such an assessment may prove to be either too involved for industrial applications because it requires a detailed knowledge about the robotic mechanics or too difficult to visualize.

This paper describes development of a kinematic error mapping facility for precision robotic operations such as a tight-tolerance assembly. The facility is based on a CAD system which models and displays the robot geometry along with its 3D working envelope. The manufacturer-specified robot manufacture tolerances are used in conjunction with the CAD geometrical database to predict the distribution of the end-effector errors over the working volume. The system features the capability of constructing and displaying a 3D error map for the feasible locations such that the location(s) with the minimum inaccuracy can be easily visualized and evaluated. The facility is based on a "low cost" CAD package (AutoCAD) suitable for operation on a personal computer and the built-in AutoLisp language is fully made use of to automate graphics and facilitate error model calculations. Both the linearized or nonlinear models are used and compared. The functionality of the system is illustrated with reference to a revolute 4-axis robot and the development of a robotic material handling workcell. The results show the system is very effective and straightforward to use, and it is considered that this system, based on a personal computer hardware platform, will generate significant interest from industry.

2. ERROR MODELS

To develop a kinematic error mapping facility, a proper mathematical model is required. The model relates the errors in kinematic parameters to the end-effector errors with respect to the world coordinate system. The model should be accurate yet computationally efficient. Both the nonlinear and linearized models are briefly reviewed and their comparison is given in a case study presented in a later section.

2.1. *Nonlinear error models*

It is well-known[16] that the relationship between links i and $i-1$ can be described by a homogeneous transformation known as the Denavit–Hartenberg matrix as

$$\mathbf{A}_i = \begin{bmatrix} \cos q_i & -\sin q_i \cos a_i & \sin q_i \sin a_i & l_i \cos q_i \\ \sin q_i & \cos q_i \cos a_i & -\cos q_i \sin a_i & l_i \sin q_i \\ 0 & \sin a_i & \cos a_i & r_i \\ 0 & 0 & 0 & 1 \end{bmatrix} \tag{1}$$

where q_i is the ith joint angle, r_i the axial offset along the ith axis of joints, l_i the common normal distance, and a_i the twist angle between joints i and $i+1$. The position and orientation of the end-effector, $\mathbf{T}_N$, is given by the multiplication of the D–H matrices along the kinematic chain

$$\mathbf{T}_N = \mathbf{A}_1 * \mathbf{A}_2 \ldots * \mathbf{A}_N \tag{2}$$

where N is the degree of freedom of the robot and $\mathbf{T}_N$ is known as the (forward) kinematics of a robot and is a 4 by 4 matrix of the following form,

$$\mathbf{T}_N = \begin{bmatrix} \mathbf{n} & \mathbf{o} & \mathbf{a} & \mathbf{p} \\ 0 & 0 & 0 & 1 \end{bmatrix}. \tag{3}$$

Assuming the kinematic errors Δl_i, Δr_i and Δa_i for a perfect revolute joint, that is $\Delta q_i = 0$, the ideal $\mathbf{A}_i$ matrix becomes:

$$\mathbf{A}_i + d\mathbf{A}_i = \begin{bmatrix} \cos q_i & -\sin q_i \cos(a_i + \Delta a_i) & \sin q_i \sin(a_i + \Delta a_i) & (l_i + \Delta l_i)\cos q_i \\ \sin q_i & \cos q_i \cos(a_i + \Delta a_i) & -\cos q_i \sin(a_i + \Delta a_i) & (l_i + \Delta l_i)\sin q_i \\ 0 & \sin(a_i + \Delta a_i) & \cos(a_i + \Delta a_i) & r_i + \Delta r_i \\ 0 & 0 & 0 & 1 \end{bmatrix} \tag{4}$$

therefore

$$\mathbf{T}_N + d\mathbf{T}_N = (\mathbf{A}_1 + d\mathbf{A}_1) * (\mathbf{A}_2 + d\mathbf{A}_2) \ldots (\mathbf{A}_{N-1} + d\mathbf{A}_{N-1}) * (\mathbf{A}_N + d\mathbf{A}_N) \tag{5}$$

where $d\mathbf{T}_N$ includes the positional and orientational errors with respect to the world coordinate system and is a 4 by 4 matrix of the following form,

$$d\mathbf{T}_N = \begin{bmatrix} d\mathbf{n} & d\mathbf{o} & d\mathbf{a} & d\mathbf{p} \\ 0 & 0 & 0 & 1 \end{bmatrix}. \tag{6}$$

2.2. *Linearized error models*

Many linearized models have been proposed. A widely accepted formation is based on Refs. 7–9, which is briefly outlined below. The positioning error $d^N = [\Delta x^N, \Delta y^N, \Delta z^N]^T$ and the orientation error $\delta^N = [\delta x^N, \delta y^N, \delta z^N]^T$, both with respect to the end-effector coordinate system, can be expressed as

$$\begin{bmatrix} \mathbf{d}^N \\ \boldsymbol{\delta}^N \end{bmatrix} = \begin{bmatrix} \mathbf{M}_1 \\ \mathbf{M}_2 \end{bmatrix} \Delta\mathbf{q} + \begin{bmatrix} \mathbf{M}_2 \\ 0 \end{bmatrix} \Delta\mathbf{r} + \begin{bmatrix} \mathbf{M}_3 \\ 0 \end{bmatrix} \Delta\mathbf{l} + \begin{bmatrix} \mathbf{M}_4 \\ \mathbf{M}_1 \end{bmatrix} \Delta\mathbf{a} \tag{7}$$

where $\Delta\mathbf{q}$, $\Delta\mathbf{r}$, $\Delta\mathbf{l}$, and $\Delta\mathbf{a}$ are N by 1 kinematic error vectors. For a revolute joint, $\Delta\mathbf{q}$ is known as the positional error, including encoder reading errors, gear train backlash, and joint clearance, while the other three are dimensional errors mainly due to manufacturing tolerance. d^N and δ^N, which are with respect to the end-effector coordinate system, can be

transformed to be with respect to the world coordinate system. For instance, the following holds if only positional errors are considered

$$[d\mathbf{p}] = \begin{bmatrix} dp_x \\ dp_y \\ dp_z \end{bmatrix} = \mathbf{n}\Delta\mathbf{x}^N + \mathbf{o}\Delta\mathbf{y}^N + \mathbf{a}\Delta\mathbf{z}^N \qquad (8)$$

where **n**, **o** and **a** are obtained from Eq.(3) and the $d\mathbf{p}$ is with respect to the world coordinate system.

2.3. *Other error models*

The four kinematic errors were found to be inadequate when defining parallel or near parallel joints. An extra term was included which is an extra rotation to compensate for the parallel and near parallel joints.[8] The new model describes the differential rotation vector and the differential change in the Cartesian position of the end-effector as a function of the five kinematic errors for each link. The $\mathbf{A}_i$ matrices were post multiplied by an additional rotation Rot(y, β_i). A linearized model including the second order nonlinear effects was also proposed.[14] From the brief review above, it is seen that for the purpose of error mapping, linearized models do not offer much advantage over the nonlinear models due to the fact that only forward kinematics are involved. However, both the nonlinear and linearized models were used to develop the error mapping facility and their comparison is presented in a later section.

3. ERROR MAPPING FACILITY

3.1. *Kinematic error map*

Using any of the error models discussed above, the end-effector errors with respect to the world coordinate system can be calculated. Since these errors are a function of the configuration of a robot, that is, a function of the end-effector location, an error map that displays the distribution of errors within the locations being considered for precision operations provides a vivid representation of the error distribution and subsequently facilitates a planner to evaluate and choose proper locations for a given operation. An error mapping facility can be readily implemented by using a modern CAD system, where the geometric database contains all necessary information concerning robot kinematics as well as kinematic errors, while the built-in language can easily implement an algorithm based on one of the error models.

Figure 1 depicts a simple 3D error map where the worktable is partitioned by a grid and the nodes on the table represent the possible location for carrying out a given precision task. The encircled nodes indicate the points where the robot cannot reach, that is, the points outside the robot working envelope. The arrows represent the extent of the deviation of the actual location from the ideal location. Errors are displayed in their three orthogonal components or as a resultant (Fig. 2).

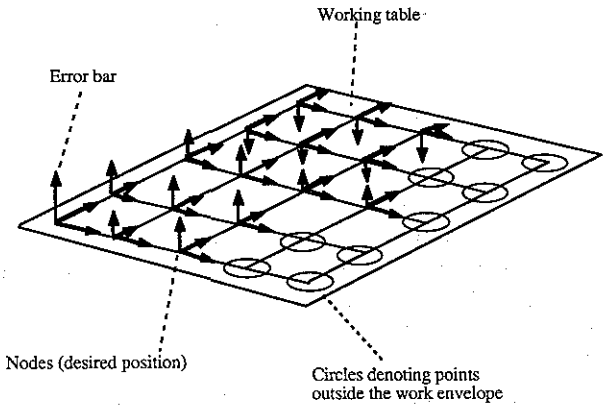

Fig. 1. Graphical representation of the errors at the end-effector.

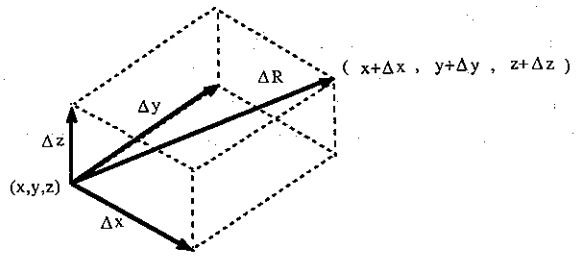

Fig. 2. The ideal and actual location.

3.2. *AutoLISP*

The CAD system used to develop the error mapping facility is AutoCAD running on a PC. It is widely available and inexpensive. Its built-in programming language, AutoLISP, is capable of accessing the CAD database with ease and makes it an ideal tool for building the error mapping facility.

AutoLISP, like other programming languages, is capable of carrying out most arithmetic and logical calculation, looping, conditional IF statement. One of the AutoLISP's major features is its capability to combine drawing commands with AutoCAD. These commands allow the programmer to automatically generate a particular drawing in AutoCAD.

In AutoCAD, the user is able to draw the objects directly from the keyboard or menu. The command prompt requires the user to input the command.

eg:

```
Command: LINE
From point: 0,32,46
To point: 42,70,65
To point: ⟨return⟩
```

A line will then be drawn from the two coordinates shown above. However, this procedure can also be done automatically via AutoLISP. A sample program duplicating the above task is given below:

```
(defun line1 ( ); to define the program
    (setq pt1 (list 0 32 46))
    (command "line" pt1'(42 70 65))
```

The sample seems trivial; however, the advantages of using AutoLISP are obvious if a complex object is involved, and the object has to be modified slightly and displayed repeatedly for evaluation, comparison or re-layout purposes.

3.3. *Layout and planning aid*

The error mapping module, as part of a computer-aided layout and planning facility, is integrated into the facility by using the capabilities of AutoCAD and AutoLISP described above. A flowchart is shown in Fig. 3. After specifying the initial end-effector location, the facility solves the robot inverse kinematics and displays the robot configuration using the geometry data stored in a library. The user then has the option of superposing the working envelope on the display. At this stage, the kinematic errors have to be fetched from the library, which are often based on the manufacturer's tolerance data. Either the nonlinear or linearized model described in the last section is used to calculate the error distribution at the end-effector. The distribution is then displayed, along with the robot and other equipment such as a conveyer, to aid layout and planning activities.

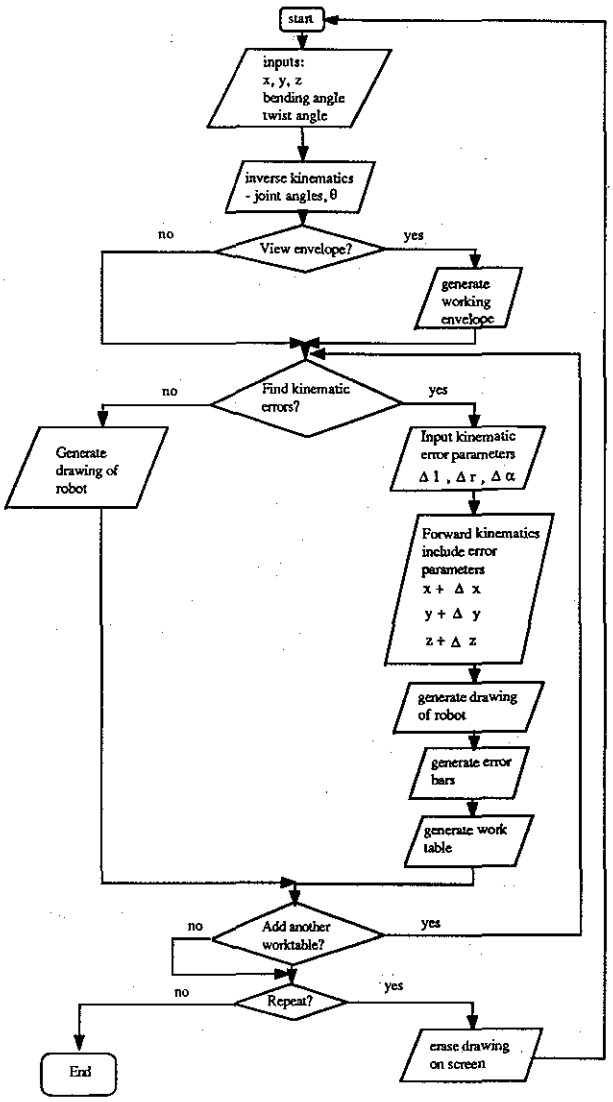

Fig. 3. Flowchart of the mathematical error models.

4. CASE STUDY

4.1. *The Hitachi PW 10–II robot*

A revolute Hitachi PW 10–II robot is used as an example to implement the error mapping facility, whose kinematic parameters have the values shown in Table 1. Its joint angles have the following limits: $-150° < q_1 < 150°$, $-45° < q_2 < 50°$, $-25° < q_3 < 45°$, and $-85° < q_4 < 95°$.

4.2. *Implementation of the error mapping facility*

As shown in Fig. 4, the geometric information of the robot is fetched from the CAD database and used to develop a wire frame model along with its working envelope. A worktable is then placed in a possible location whose desktop must intersect with the working volume. The top surface is partitioned by a 9 by 10 grid with the intersect points known as nodes. Some node points are encircled to indicate they are outside the working envelope and therefore are immediately excluded from consideration because they are obviously non-feasible.

To demonstrate the construction of an error map, the kinematic errors shown in Table 2 are used as an example. In reality, these errors can be assigned based on manufacturer's tolerance data. Using the error

Table 1. Ideal values of the kinematic parameters for the Hitachi PW 10–II robot

Link No.	q (degrees)	l (mm)	r (mm)	a (degrees)
1	q_1	0	750.0	90.0
2	q_2	600.0	0	0
3	q_3	850.0	0	0
4	q_4	400.0	0	0

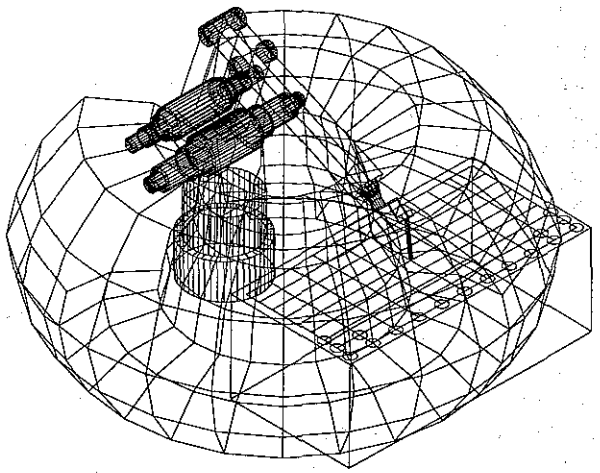

Fig. 4. Working envelope and working table (circles denote nodes out of the work envelope).

Table 2. Values of kinematic errors for the example

Link No.	Δl (mm)	Δr (mm)	Δa (degrees)
1	1.0	3.0	1.0°
2	3.0	1.0	0.5°
3	4.0	1.0	1.0°
4	0	1.0	1.0°

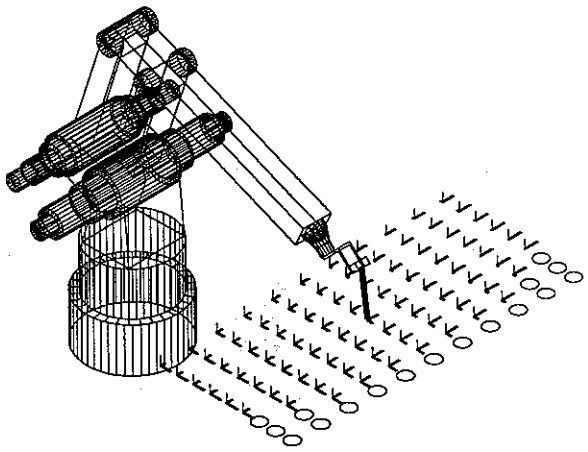

Fig. 5. An error map.

models described in Section 2 above, the end-effector errors are calculated. For simplicity of graphical presentation, this example only includes translational errors, that is, Δx, Δy, and Δz. These errors are calculated for every feasible node points and their values are represented by the length of the arrows (Fig. 5). This provides a vivid picture of the error distribution on the table top which is being considered for a precision task. The resultant of these errors can also be displayed (Fig. 6).

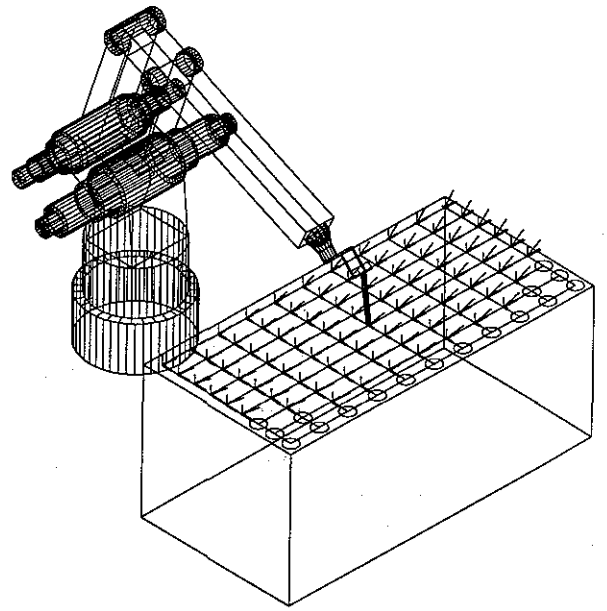

Fig. 6. An error map with the resultant error.

Points with the minimum error in various senses are then found, such as in the sense of the minimum error in the x-, y-, or z-direction, or in the sense of the minimum error of the resultant in the x–y plane or the 3D resultant. Which sense to choose depends on applications, for example, the point with the minimum error of the resultant in the x–y plane will be chosen as an ideal location for precision assembly operations where the error in the z-direction is unimportant during part mating. The error mapping facility can be extended to include other equipment such as a conveyor shown in Fig. 7.

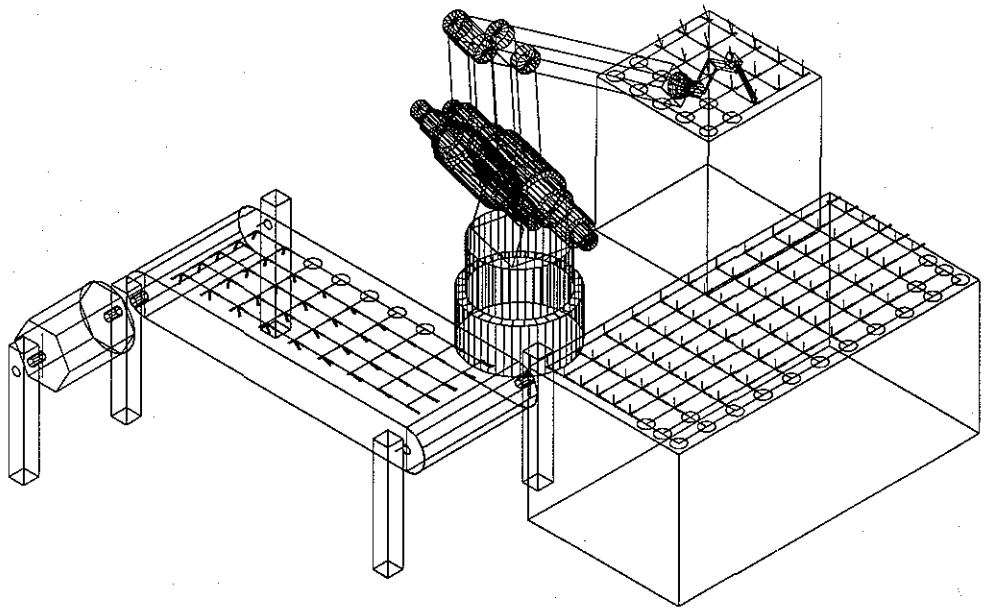

Fig. 7. Error maps for a robotic workcell.

Table 3. Values of kinematic errors for comparison

Link No.	Δl (mm)	Δr (mm)	Δa (degrees)
1	1.0	1.0	0.5°
2	1.0	1.0	0.3°
3	1.0	1.0	0.5°
4	1.0	1.0	0.5°

4.3. *Comparison between the nonlinear and the linearized error models*

For the comparative reason, both the nonlinear and linearized error models were used to determine the end-effector errors. The data used were:

- Initial end-effector position = (0,1250,1350) mm and initial tool bending angle = 0°;
- Size of working table = 1500 mm (in x direction) by 700 mm (in y direction);
- Number of divisions on the grid, $m = 10$ (in x direction) by $n = 8$ (in y direction);
- The number of node points = $(m + 1)(n + 1) = 11*9 = 99$ and the kinematic error values are listed in Table 3.

The discrepancy between using the nonlinear and the linearized error models are characterised by calculating the percentage discrepancy as follows:

$$D_i(\%) = \frac{\text{ABS}(\Delta_{iNL} - \Delta_{iL})}{\text{ABS}(\Delta_{iNL})} \quad i = x, y, z, \text{and } r \qquad (9)$$

where Δ_{iNL} and Δ_{iL} are the end-effector errors calculated using the nonlinear and the linearized error models, respectively. ABS denotes absolute value and r the resultant. D_i for ($i = x, y, z$, and r) are plotted in Fig. 8.

4.4. *Discussions*

From the comparison between using the nonlinear and linearized error models, it is seen that the discrepancy introduced by the linearization is negligible. Of course, the discrepancy is again a function of the robot configuration. But no discrepancy more than 1% was observed for any node points (Fig. 8). It is due to the fact that the kinematic errors are normally very small deviations from the nominal dimensions such that the assumption of the linearization generally holds.

The case study shows that the facility is extremely flexible. Not only various robots, but also other equipment, such as working tables and conveyors, can be stored and called upon from a library and placed within the robot working envelope. Then error maps can be constructed on all locations being considered for robot operations and the spot(s) with the minimum errors in a sense consistent with the nature of the operation can be chosen. In order to do so, knowledge of the robot kinematic errors is required which is at times not readily available. Possible sources of such information include manufacturer's specifications of tolerance or through calibration.

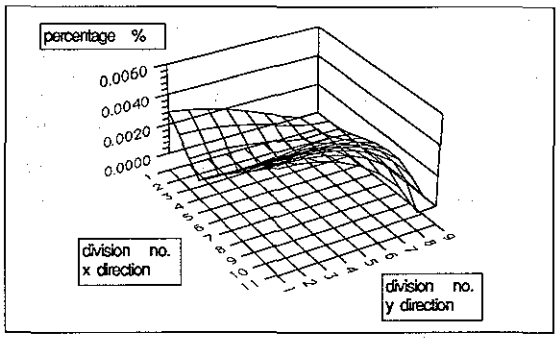

a) Discrepancy in x Direction

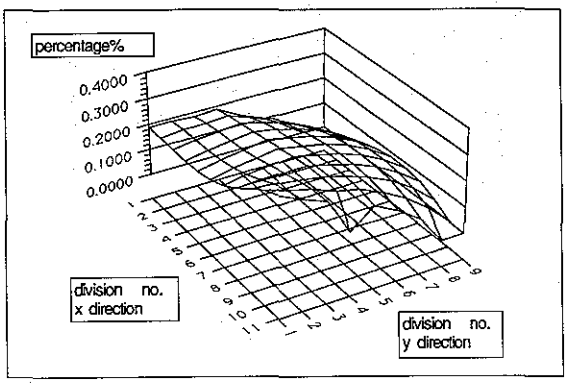

b) Discrepancy in y Direction

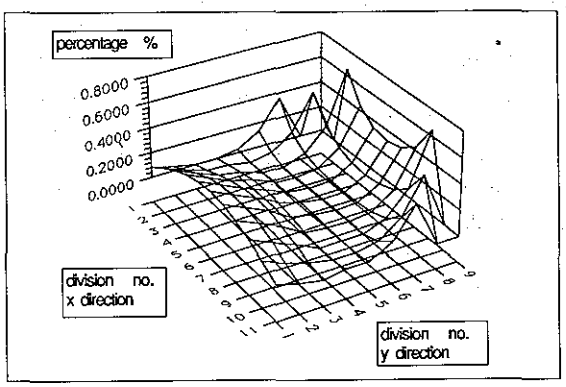

c) Discrepancy in z Direction

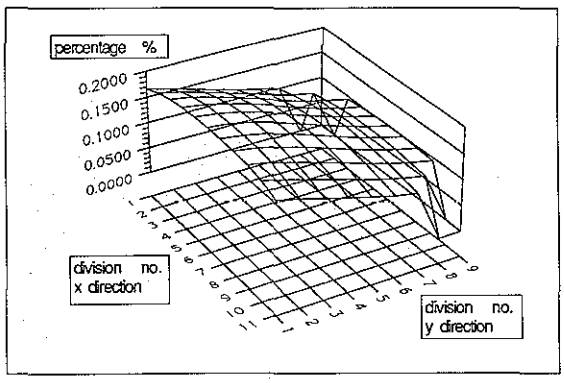

d) Discrepancy in the Resultant

Fig. 8. Percentage discrepancy between using nonlinear and linearized error models [number of divisions of the grid, $m = 10$ (in x direction) by $n = 8$ (in y direction); number of node points = $(m + 1)(n + 1) = 11*9 = 99$].

5. CONCLUSIONS

The error mapping facility is proven to be a useful aid in the layout and planning of robotic operations where positioning accuracy is a major concern. The facility, built upon a popular PC-based CAD system, takes full advantages of the geometry database and sophisticated graphics capability of the CAD system. The built-in programming language of the system allows automation of both error model calculation and graphics updating thus permitting extensive evaluation of various options which is essential in reaching a better solution at the layout and planning stage. It certainly reduces the need for trial-and-error experiments to determine the optimum position which may be very time consuming and may involve high technical risks. Both nonlinear and linearized error models are used in the facility and the results show little discrepancy between them due to the fact that the kinematic errors are small deviations from their nominal values only. The facility may also provide useful information for the case where a robot's accuracy is inadequate for a given task and utilization of additional devices or sensors becomes necessary.

REFERENCES

1. Fougere, T. J., Kanerva, J. J.: ROBOT-SIM: a CAD based workcell design and off-line programming system. *Proceedings of ROBOTS 10*, SME, 1986, Ch. 7, pp. 1–13.
2. Hoang, K. *et al.*: Optimum location of robots in FMS work cell. *Proceedings of 4th International Conference on Manufacturing Engineering*, Brisbane, 11–13 May 1988, pp. 88–92.
3. Hoang, K. *et al.*: Computer-aided layout of robots in manufacturing cells. *Proceedings of 5th International Conference on Manufacturing Engineering*, July 1990, Wollongong, Australia.
4. Mavridis, B.: An AutoCAD based robotic layout and planning facility. B.E. Thesis, Department of Mechanical Engineering, University of Wollongong, 1989.
5. Whitney, D. E., Lozinski, C. A., Rourke, J. M.: Industrial robot forward calibration method and results. *ASME Trans. J. Dynamic Systems Measurement Control* **108**: 1–8, Mar. 1986.
6. Shamma, J. S., Whitney, D. E.: A method for inverse robot calibration. *ASME Trans. J. Dynamic Systems Measurement Control* **109**: 36–43, Mar. 1987.
7. Wu, C.-H.: The kinematic error model for the design of robot manipulator. *American Control Conference*, June 1983, pp. 497–502.
8. Wu, C.-H., Lee, C. C.: Estimation of the accuracy of robot manipulator. *IEEE Trans, Automatic Control* AC-**30** (3): 304–306, 1985.
9. Wu, C.-H.: A kinematic CAD tool for the design and control of robot manipulator. *Int. J. Robotics Res.* **3** (1): 58–67, Spring 1984.
10. Wu, C.-H., Vietschegger, W. K.: Robot accuracy analysis based on kinematics. *IEEE J. Robotics Automation* RA-**2** (3): 171–179, Sept. 1986.
11. Mooring, B. W., Padavala, S. S.: The effect of kinematic model complexity on manipulator accuracy. *Proceedings of IEEE International Conference on Robotics and Automation*, 1989, pp. 593–598.
12. Borm, J.-H., Menq, C.-H.: Experimental study of observability of parameter errors in robot calibration. *Proceedings of IEEE International Conference on Robotics and Automation*, pp. 587–592.
13. Bennett, D. J., Hollerbach, J. M.: Identifying the kinematics of robots and their tasks. *Proceedings of IEEE International Conference on Robotics and Automation*, 1989, pp. 580–586.
14. Ahmad, S.: Second order nonlinear kinematic effects, and their compensation. *Proceedings of IEEE International Conference on Robotics and Automation*, 1985, pp. 307–314.
15. Kumar, A., Waldron, K. J.: Numerical plotting of surfaces of positioning accuracy of manipulators. *Mechanism Machine Theory* **16** (4): 361–368, 1981.
16. Paul, R. P.: *Robot Manipulators: Mathematics, Programming and Control*, Cambridge, MA, M.I.T. Press, 1981.